Uniform hopping approach to the ferromagnetic Kondo model at finite temperature

Winfried Koller,* Alexander Prüll, Hans Gerd Evertz, and Wolfgang von der Linden
Institut für Theoretische Physik, Technische Universität Graz, Petersgasse 16, A-8010 Graz, Austria
(Received 29 November 2002; published 31 March 2003)

We study the ferromagnetic Kondo model with classical corespins via unbiased Monte Carlo simulations and derive a simplified model for the treatment of the core spins at any temperature. Our simplified model captures the main aspects of the Kondo model and can easily be evaluated both numerically and analytically. It provides a better qualitative understanding of the physical features of the Kondo model and rationalizes the Monte Carlo results including the spectral density $A_k(\omega)$ of a one-dimensional (1D) chain with nearest-neighbor Coulomb repulsion. By calculating the specific heat and the susceptibility of systems up to size 16^3, we determine the Curie temperature of the 3D one-orbital double-exchange model, which agrees with experimental values.

DOI: 10.1103/PhysRevB.67.104432 PACS number(s): 75.10.−b, 75.30.Kz, 71.10.−w

I. INTRODUCTION

Manganese oxides such as $La_{1-x}Sr_xMnO_3$ and $La_{1-x}Ca_xMnO_3$ have been attracting considerable attention since the discovery of colossal magnetoresitance.[1,2] These materials crystallize in the perovskite-type lattice structure, where the crystal field breaks the symmetry of the atomic wave function of the manganese d electrons. The energetically lower t_{2g} levels are occupied by three localized electrons. Due to a strong Hund coupling, their spins are aligned, thus forming a localized corespin with $S=3/2$. The electron configuration of the Mn^{3+} ions is $t_{2g}^3 e_g^1$, whereas for Mn^{4+} ions the e_g electron is missing. Due to a hybridization of the e_g wave function with the oxygen $2p$ orbitals, the e_g electrons are itinerant and can move from an Mn^{3+} ion to a neighboring Mn^{4+} via a bridging O^{2-}. The interplay of various physical ingredients such as the strong Hund coupling of the itinerant electrons to localized corespins, Coulomb correlations, and electron-phonon coupling leads to a rich phase diagram including antiferromagnetic insulating, ferromagnetic metallic, and charge ordered domains. The carriers moving in the spin and orbital background show remarkable dynamical features.[3,4]

Since full many-body calculations for a realistic model, including all degrees of freedom, are not possible yet, several approximate studies of simplified models have been performed in order to unravel individual pieces of the rich phase diagram of the manganites. The electronic degrees of freedom are generally treated by a Kondo lattice model, which in the strong Hund coupling limit is commonly referred to as the double-exchange (DE) model, a term introduced by Zener.[5] In addition, the correlation of the itinerant e_g electrons is well described by a nearest-neighbor (nn) Coulomb interaction. The on-site Hubbard term merely renormalizes the already strong Hund coupling. For the Kondo model with quantum spins, it is still impossible to derive rigorous numerical and analytical results. If the $S=3/2$ corespins are treated classically, however, the model can be treated by unbiased Monte Carlo techniques. The impact of quantum spins on the electronic properties has been studied in Refs. 6–8. It appears that quantum effects are important for $S=1/2$ corespins or at $T=0$. For finite temperature and $S=3/2$, classical spins present a reasonable approximation.

Elaborate Monte Carlo (MC) simulations for the ferromagnetic (FM) Kondo model with classical t_{2g} corespins have been performed by Dagotto *et al.*,[9–11] Yi *et al.*,[12] Furukawa,[13] and Motome and Furukawa.[14] Static and dynamical properties of the model have been determined. These studies revealed features that have been interpreted as signatures of phase separation (PS). PS has also been reported[15] from computations based on a dynamical mean-field treatment of the DE model at $T=0$. A phase diagram and critical exponents of the DE model have been determined with a hybrid MC algorithm.[16,17]

In the manganites, the Hund coupling J_H is much stronger than the kinetic energy. Consequently, configurations are very unlikely in which the electronic spin is antiparallel to the local corespin. It is therefore common practice to use $J_H=\infty$ and to ignore antiparallel spin arrangements altogether. This approximation yields reasonable results in the ferromagnetic regime. Close to half filling, however, a finite ferromagnetic Hund coupling even enhances the antiferromagnetic ordering of the corespins. In a previous paper,[18] we have proposed an effective spinless fermion (ESF) model that takes effects of antiparallel $t_{2g}-e_g$ spin configurations into account via virtual excitations. It has been demonstrated that the results of the ESF model are in excellent agreement with those of the original Kondo model even for moderate values of J_H.

In Ref. 18, we also introduced the uniform hopping approach (UHA), which replaces the influence of the random corespins on the e_g electron dynamics by an effective uniform hopping process. In that work, the hopping parameter was determined by minimization of the ground-state energy. Essential physical features of the original model could be described even quantitatively by UHA, while the configuration space, and hence the numerical effort, was reduced by several orders of magnitude. Besides the numerical advantage, UHA also allows the derivation of analytical results in some limiting cases.

In the present paper, we extend the UHA to finite temperature. Thermal fluctuations of the corespins are mapped to fluctuations of the uniform hopping parameter. In order to include entropy effects correctly, we have to determine the density $\Gamma(u)$ of corespin states for a given hopping parameter u. The reliability of the finite-temperature UHA is scrutinized by a detailed comparison of the results for various

properties of the one-orbital DE model with unbiased MC data.

So far, in most MC simulations, the Coulomb interaction of the e_g electrons has been neglected due to its additional computational burden. It should, however, have an important impact, particularly on phase separation. Moreover, at quarter filling, the nn repulsion leads to the charge ordering (CO) phase. We have performed MC simulations for the Kondo model including a Hubbard-like Coulomb interaction. In these simulations, for each classical corespin configuration, the electronic degrees of freedom are treated by Lanczos exact diagonalization. We find that also in this case UHA yields reliable results while reducing the computational complexity by orders of magnitude. An excerpt of the results is given here, while a thorough discussion will be provided elsewhere.

Also starting from an UHA-type of Hamiltonian, Millis *et al.*[19] claim that the bare DE model cannot even explain the right order of magnitude of the Curie temperatures of the manganites. This claim is, however, based on uncontrolled additional approximations. We find that a more rigorous evaluation of UHA for a one-orbital DE model and large three-dimensional (3D) systems yields a Curie temperature which is indeed close to the experimental values. Our results for the DE model are in accord with the Hybrid MC result[17] and with other estimates.[11,13,20]

This paper is organized as follows. In Sec. II, the model Hamiltonian is presented and particularities of the MC simulation are outlined. The uniform hopping approach is discussed in Sec. III. One-dimensional applications are given in Sec. IV and compared with MC data. The impact of Coulomb correlations on the spectral density is discussed. In Sec. V, the UHA is used to calculate the phase diagram of the DE model in three dimensions. The key results of the paper are summarized in Sec. VI.

II. MODEL HAMILTONIAN AND UNBIASED MONTE CARLO SIMULATION

In this paper, we will concentrate on properties of the itinerant e_g electrons interacting with the local t_{2g} corespins. It is commonly believed that the electronic degrees of freedom are well described by a multiorbital Kondo lattice model

$$\hat{H}=-\sum_{\substack{ij\alpha\beta\\ \sigma}} t_{i\alpha,j\beta}a^{\dagger}_{i\alpha\sigma}a_{j\beta\sigma}-J_H\sum_{i\alpha}\boldsymbol{\sigma}_{i\alpha}\mathbf{S}_i+\sum_{ij\alpha\beta}V_{i\alpha,j\beta}\hat{n}_{i\alpha}\hat{n}_{j\beta}+J'\sum_{\langle ij\rangle}\mathbf{S}_i\cdot\mathbf{S}_j. \quad (1)$$

As proposed by de Gennes,[21] Dagotto *et al.*,[9,22] and Furukawa,[13] the t_{2g} spins $\mathbf{S}_i$ are treated classically, which is equivalent to the limit $S\to\infty$. The spin degrees of freedom are thus replaced by unit vectors $\mathbf{S}_i$, parametrized by polar and azimuthal angles θ_i and ϕ_i, respectively. The magnitude of both corespins and e_g spins is absorbed into the exchange couplings.

Equation (1) consists of a kinetic term for the itinerant e_g electrons with transfer integrals $t_{i\alpha,j\beta}$, where $i(j)$ are site indices, $\alpha(\beta)$ orbital indices, and $\sigma(\sigma')$ spin indices. The transfer integrals, which are restricted to nn sites, are given as matrices in the orbital indices $\alpha,\beta=1(2)$ for x^2-y^2 $(3z^2-r^2)$ orbitals (see e.g., Ref. 22),

$$t_{i,i+\hat{z}}=t\begin{pmatrix}0&0\\0&1\end{pmatrix},\quad t_{i,i+\hat{x}/\hat{y}}=t\begin{pmatrix}\frac{3}{4}&\mp\frac{\sqrt{3}}{4}\\ \mp\frac{\sqrt{3}}{4}&\frac{1}{4}\end{pmatrix}. \quad (2)$$

The overall hopping strength is t, which will be used as unit of energy, by setting $t=1$. The operators $a^{\dagger}_{i\alpha\sigma}(a_{i\alpha\sigma})$ create (annihilate) e_g electrons at site x_i in orbital α with spin σ. The second term of the Hamiltonian describes the Hund coupling with exchange integral J_H, where $\vec{\sigma}_{i\alpha}$ stands for the spin of the electron at site i in orbital α. The spin-resolved occupation number operator is denoted by $\hat{n}_{i\alpha\sigma}$. The third term describes a Coulomb repulsion, with $\hat{n}_{i\alpha}$ being the spin-integrated density operator. The local Hubbard interaction is excluded from the sum, i.e., $V_{i\alpha,i\alpha}=0$, as it effectively merely modifies the Hund coupling J_H. Finally, Eq. (1) contains a superexchange term. The value of the exchange coupling is $J'\approx 0.02$,[22] accounting for the weak antiferromagnetic coupling of the t_{2g} electrons.

For strong Hund coupling $J_H\gg t$, the electronic density of states (DOS) essentially consists of two sub-bands, a lower and an upper Kondo band, split by $\approx 2J_H$. In the lower band, the itinerant e_g electrons move such that their spins are predominantly parallel to the t_{2g} corespins, while the opposite is true for the upper band.[23] Throughout this paper, the electronic density n (number of electrons per orbital) will be restricted to $0\leqslant n\leqslant 1$, i.e., only the lower Kondo band is involved.

A. Effective spinless fermions

It is expedient to use the individual t_{2g} spin directions $\mathbf{S}_i$ as the local quantization axes for the spin of the itinerant e_g electrons at the respective sites. This representation is particularly useful for the $J_H\to\infty$ limit, but also for the projection technique, which takes into account virtual processes for finite Hund coupling. The transformation in the electronic spin is described by a local unitary 2×2 matrix $U(\mathbf{S}_i)$ with

$$\vec{a}_{i\alpha}=U(\mathbf{S}_i)\vec{c}_{i\alpha}\quad \vec{c}_{i\alpha}=U^{\dagger}(\mathbf{S}_i)\vec{a}_{i\alpha}, \quad (3)$$

where $\vec{a}_{i\alpha}$ is a column vector with entries $a_{i\alpha\uparrow}$ and $a_{i\alpha\downarrow}$, respectively. The transformed annihilation operators in local quantization are represented by $\vec{c}_{i\alpha}$. For the creation operators, we have

$$\vec{a}^{\dagger}_{i\alpha}=\vec{c}^{\dagger}_{i\alpha}U^{\dagger}(\mathbf{S}_i),\quad \vec{c}^{\dagger}_{i\alpha}=\vec{a}^{\dagger}_{i\alpha}U(\mathbf{S}_i). \quad (4)$$

The unitary matrix $U(\mathbf{S}_i)$ depends upon $\mathbf{S}_i$ and is chosen such that it diagonalizes the individual contributions to the Kondo exchange

$$\boldsymbol{\sigma}_{i\alpha}\mathbf{S}_i \equiv \vec{a}^{\dagger}_{i\alpha}(\boldsymbol{\Sigma}\mathbf{S}_i)\vec{a}_{i\alpha} = \vec{c}^{\dagger}_{i\alpha}(U^{\dagger}(\mathbf{S}_i)(\boldsymbol{\Sigma}\mathbf{S}_i)U(\mathbf{S}_i))\vec{c}_{i\alpha}, \quad (5)$$

with $\boldsymbol{\Sigma}$ being the vector of Pauli matrices. The eigenvalues of $(\boldsymbol{\Sigma}\mathbf{S}_i)$ are ± 1 and the matrix of eigenvectors is given by

$$U(\mathbf{S}_i) = \begin{pmatrix} c_i & s_i e^{-i\phi_i} \\ s_i e^{i\phi_i} & -c_i \end{pmatrix}, \quad (6)$$

with the abbreviations $c_j = \cos(\theta_j/2)$ and $s_j = \sin(\theta_j/2)$ and the restriction $0 \leqslant \theta_j \leqslant \pi$. The Kondo exchange term in Eq. (5) in the new representation reads

$$\boldsymbol{\sigma}_{i\alpha}\mathbf{S}_i = \hat{n}_{i\alpha\uparrow} - \hat{n}_{i\alpha\downarrow}. \quad (7)$$

The spin-integrated density operators $\hat{n}_{i\alpha}$ are unaffected by the unitary transformation. The entire Kondo Hamiltonian becomes

$$\hat{H} = -\sum_{\substack{ij\alpha\beta \\ \sigma\sigma'}} t^{\sigma,\sigma'}_{i\alpha,j\beta} c^{\dagger}_{i\alpha\sigma} c_{j\beta\sigma'} + 2J_H \sum_{i\alpha} \hat{n}_{i\alpha\downarrow} + \sum_{ij\alpha\beta} V_{i\alpha,j\beta} \hat{n}_{i\alpha}\hat{n}_{j\beta} + J' \sum_{\langle ij\rangle} \mathbf{S}_i \cdot \mathbf{S}_j. \quad (8)$$

We have added an additional term $\hat{H}_c = J_H \hat{N}$ proportional to the e_g-electron number N, equivalent to a trivial shift of the chemical potential.

The prize to be paid for the simple structure of the Hund term is that the modified hopping integrals $t^{\sigma,\sigma'}_{i\alpha,j\beta}$ now depend upon the t_{2g} corespins,

$$t^{\sigma,\sigma'}_{i\alpha,j\beta} = t_{i\alpha,j\beta}(U^{\dagger}(\mathbf{S}_i)U(\mathbf{S}_j))_{\sigma,\sigma'} = t_{i\alpha,j\beta} u^{\sigma,\sigma'}_{ij}. \quad (9)$$

The relative orientation of the t_{2g} corespins at site i and j enters via

$$u^{\sigma,\sigma}_{i,j}(\mathcal{S}) = c_i c_j + s_i s_j e^{i\sigma(\phi_j - \phi_i)} = \cos(\vartheta_{ij}/2) e^{i\psi_{ij}}$$
$$u^{\sigma,-\sigma}_{i,j}(\mathcal{S}) = \sigma(c_i s_j e^{-i\sigma\phi_j} - c_j s_i e^{-i\sigma\phi_i}) \sin(\vartheta_{ij}/2) e^{i\chi_{ij}} \quad (10)$$

These factors depend on the relative angle ϑ_{ij} of corespins $\mathbf{S}_i$ and $\mathbf{S}_j$ in the corespin configuration $\mathcal{S}$ and on some complex phases ψ_{ij} and χ_{ij}. It should be noticed that the modified hopping part of the Hamiltonian is still Hermitian because $u^{\sigma,\sigma'}_{i,j} = (u^{\sigma',\sigma}_{j,i})^*$.

The advantage of the local quantization is, as described in Ref. 18, that the energetically unfavorable states with e_g electrons antiparallel to the local t_{2g} corespins can be integrated out. This leads to the effective spinless fermion model

$$\hat{H}_p = -\sum_{i,j,\alpha,\beta} t^{\uparrow\uparrow}_{i\alpha,j\beta} c^{\dagger}_{i\alpha} c_{j\beta} - \sum_{i,j,\alpha,\beta,\alpha'} \frac{t^{\uparrow\downarrow}_{i\alpha',j\beta} t^{\downarrow\uparrow}_{j\beta,i\alpha}}{2J_H} c^{\dagger}_{i\alpha'} c_{i\alpha} + \sum_{ij\alpha\beta} V_{i\alpha,j\beta} \hat{n}_{i\alpha}\hat{n}_{j\beta} + J' \sum_{\langle ij\rangle} \mathbf{S}_i \cdot \mathbf{S}_j. \quad (11)$$

The spinless fermion operators correspond to spin-up electrons (relative to the *local* corespin-orientation) only. The spin index has therefore been omitted. With respect to a *global* spin-quantization axis, the ESF model (11) still contains contributions from both spin-up and spin-down electrons. The V-dependent contributions in the energy denominator have been ignored, since $|V_{i\alpha,j\beta}| \ll |J_H|$. In principle, the effective Hamiltonian also contains ''three-site'' hopping processes. It has been shown[18] that the three-site term has negligible impact, and it has been ignored here.

Since each eigenvector can have an arbitrary phase, the unitary matrix in Eq. (6) is not unique. This implies that

$$U(S_i) = \begin{pmatrix} c_i & s_i e^{-i\phi_i} \\ s_i e^{i\phi_i} & -c_i \end{pmatrix} \begin{pmatrix} e^{i\alpha(i)} & 0 \\ 0 & e^{i\beta(j)} \end{pmatrix}$$

also diagonalizes the Kondo term. The additional phase factors modify the hopping integrals of the spin-up channel as

$$u^{\uparrow\uparrow}_{i,j}(\mathcal{S}) = (c_i c_j + s_i s_j e^{i(\phi_j - \phi_i)}) e^{i[\alpha(j) - \alpha(i)]} = \cos(\vartheta_{ij}/2) e^{i[\psi_{ij} + \alpha(j) - \alpha(i)]}. \quad (12)$$

Consequently, in the one-dimensional case and with open boundaries, we can choose the local phase factors such that the nn hopping integrals are simply given by the real numbers $\cos(\vartheta_{ij}/2)$.

B. Grand canonical treatment

Our model contains classical (corespins) and quantum-mechanical (e_g electrons) degrees of freedom. The appropriate way to cope with this situation in statistical mechanics is to define the grand canonical partition function as

$$\mathcal{Z} = \int \mathcal{D}[\mathcal{S}] \mathrm{tr}_c e^{-\beta[\hat{H}(\theta,\phi) - \mu\hat{N}]},$$
$$\int \mathcal{D}[\mathcal{S}] = \prod_{i=1}^{L} \left(\int_0^{\pi} d\theta_i \sin\theta_i \int_0^{2\pi} d\phi_i \right), \quad (13)$$

where tr_c indicates the trace over fermionic degrees of freedom at inverse temperature β, $\hat{N}$ is the operator for the total number of e_g electrons, L is the number of lattice sites, and μ stands for the chemical potential. Upon integrating out the fermionic degrees of freedom, we obtain the statistical weight of a corespin configuration $\mathcal{S}$

$$w(\mathcal{S}) = \frac{\mathrm{tr}_c e^{-\beta[\hat{H}(\mathcal{S}) - \mu\hat{N}]}}{\mathcal{Z}}. \quad (14)$$

Equation (13) is the starting point of Monte Carlo simulations for the Kondo model,[9] where the sum over the classical spins is performed via importance sampling. The spin configurations $\mathcal{S}$ enter the Markov chain according to the weight factor $w(\mathcal{S})$ that is computed via exact diagonalization of the corresponding Hamiltonian in Eq. (8). In the 1D case, we have performed MC simulations, in which spins in domains of random lengths were rotated. We have performed MC runs with 1000 measurements. The skip between subsequent measurements was chosen to be some hundreds of lattice sweeps reducing autocorrelations to a negligible level.

Apart from quantities that can be derived directly from the partition function $\mathcal{Z}$, we will also be interested in dy-

namical observables, notably in the one-particle retarded Green's function $\langle\langle a_{i\alpha\sigma};a^{\dagger}_{j\beta\sigma}\rangle\rangle_{\omega}$ in global spin quantization. This function follows from

$$\langle\langle a_{i\alpha\sigma};a^{\dagger}_{j\beta\sigma}\rangle\rangle_{\omega}=\int \mathcal{D}[\mathcal{S}]w(\mathcal{S})\langle\langle a_{i\alpha\sigma};a^{\dagger}_{j\beta\sigma}\rangle\rangle^{\mathcal{S}}_{\omega}. \quad (15)$$

The one-particle Green's function $\langle\langle a_{i\alpha\sigma};a^{\dagger}_{j\beta\sigma}\rangle\rangle^{\mathcal{S}}_{\omega}$, corresponding to a particular corespin configuration $\mathcal{S}$, is determined from the Green's function in local spin quantization by employing Eqs. (3) and (4):

$$\langle\langle a_{i\alpha\sigma};a^{\dagger}_{j\beta\sigma}\rangle\rangle^{\mathcal{S}}_{\omega}=U(\mathbf{S}_i)_{\sigma\uparrow}U^{*}(\mathbf{S}_j)_{\sigma\uparrow}\langle\langle c_{i\alpha};c^{\dagger}_{j\beta}\rangle\rangle^{\mathcal{S}}_{\omega}. \quad (16)$$

To arrive at Eq. (16), we used the fact that in *local* quantization only the spin-up channel contributes to $\langle\langle c_{i\alpha\sigma};c^{\dagger}_{j\beta\sigma'}\rangle\rangle^{\mathcal{S}}_{\omega}$, i.e., $\sigma=\sigma'=\uparrow$. The spin-down channel has structures corresponding to the upper Kondo band, in which we are not interested here. In *global* quantization, both spin directions contribute. The spin-integrated Green's function reads

$$\sum_{\sigma}\langle\langle a_{i\alpha\sigma};a^{\dagger}_{j\beta\sigma}\rangle\rangle^{\mathcal{S}}_{\omega}=u^{\uparrow\uparrow}_{ji}(\mathcal{S})\langle\langle c_{i\alpha};c^{\dagger}_{j\beta}\rangle\rangle^{\mathcal{S}}_{\omega}. \quad (17)$$

The unbiased Monte Carlo result for the spin-integrated one-particle Green's function is therefore determined from

$$\sum_{\sigma}\langle\langle a_{i\alpha\sigma};a^{\dagger}_{j\beta\sigma}\rangle\rangle_{\omega}=\int \mathcal{D}[\mathcal{S}]w(\mathcal{S})u^{\uparrow\uparrow}_{ji}(\mathcal{S})\langle\langle c_{i\alpha};c^{\dagger}_{j\beta}\rangle\rangle^{\mathcal{S}}_{\omega}. \quad (18)$$

We note that the one-particle DOS is independent of the choice of the spin quantization because it can be determined from diagonal Green's functions in real space.

III. UNIFORM HOPPING APPROACH AT FINITE *T*

The impact of the DE mechanism on the electronic kinetic energy can be mimicked by an *average* hopping amplitude.[21] In a previous paper,[18] we introduced what we called the uniform hopping approach (UHA). It gave strikingly good results for ground-state properties. The idea behind UHA is to replace the terms $u^{\uparrow\uparrow}_{ij}$ in the hopping amplitude, Eq. (9), which correspond to $\cos(\vartheta_{ij}/2)$ as discussed before, by a uniform value u. In Ref. 18, the optimal UHA parameter u was determined by minimizing the ground-state energy. Here, we will extend this approach to finite temperatures by taking entropic effects into account.

In order to introduce the finite-temperature UHA, we proceed as follows. For a given corespin configuration characterized by the set of angles $\{\theta_i,\phi_i\}$, we define the *average u* value

$$u(\mathcal{S})=\frac{1}{N_p}\sum_{\langle ij\rangle}u^{\uparrow\uparrow}_{ij}(\mathcal{S}).$$

Here, N_p is the number of nn pairs $\langle ij\rangle$. We now replace the individual factors $u^{\uparrow\uparrow}_{ij}$ in Eq. (13) by $u(\mathcal{S})$. Besides $u^{\uparrow\uparrow}_{ij}$, the Hamiltonian depends on $|u^{\sigma,-\sigma}_{ij}|^2$ and on $\mathbf{S}_i\cdot\mathbf{S}_j$, which correspond to $\sin^2(\vartheta_{ij}/2)$ and $\cos\vartheta_{ij}$, respectively. As a further approximation (see below), these terms are respectively replaced by $1-u^2(\mathcal{S})$ and $2\,u^2(\mathcal{S})-1$.

The introduction of UHA leads to the partition function

$$\mathcal{Z}=\int \mathcal{D}[\mathcal{S}]\int_0^1 du\,\delta(u-u(\mathcal{S}))\mathrm{tr}_c e^{-\beta[\hat{H}(u)-\mu\hat{N}]}$$

$$=:\int_0^1 du\,\Gamma_{N_p}(u)e^{-\beta\Omega(u)}. \quad (19)$$

The integrand can be interpreted as the (non-normalized) thermal probability density for the uniform hopping parameter u,

$$p(u|\beta)=\Gamma_{N_p}(u)e^{-\beta\Omega(u)}. \quad (20)$$

It consists of the density of corespin states $\Gamma_{N_p}(u)$ and the Boltzmann factor. The former corresponds to a density of states and is given by

$$\Gamma_{N_p}(u)=\int \mathcal{D}[\mathcal{S}]\,\delta(u-u(\mathcal{S})). \quad (21)$$

It accounts for the number of different corespin configurations (multiplicity) that give rise to the same average hopping amplitude u. We note that since angles $\vartheta_{ij}/2$ enter into Eq. (10), this is different from the density of states of the classical Heisenberg model. The grand potential $\Omega(u)$

$$-\beta\Omega(u)=\ln \mathrm{tr}_c e^{-\beta[\hat{H}(u)-\mu\hat{N}]} \quad (22)$$

is obtained from the fermionic trace of the homogeneous version of the Hamiltonian of Eq. (11), which reads

$$\hat{H}_p(u)=-u\sum_{\substack{\langle i,j\rangle\\ \alpha,\beta}}t_{i\alpha,j\beta}c^{\dagger}_{i\alpha}c_{j\beta}-(1-u^2)\sum_{\substack{\langle i,j\rangle\\ \alpha,\beta,\alpha'}}\frac{t_{i\alpha',j\beta}t_{j\beta,i\alpha}}{2J_H}$$

$$\times c^{\dagger}_{i\alpha'}c_{i\alpha}+\sum_{i,j,\alpha,\beta}V_{i\alpha,j\beta}\hat{n}_{i\alpha}\hat{n}_{j\beta}+J'N_p(2u^2-1). \quad (23)$$

The uniform hopping approach presents an enormous simplification of the original problem. First, the evaluation of the fermionic trace simplifies considerably; for noninteracting electrons ($V=0$), it can even be computed analytically. Second, the high-dimensional configuration space of the corespins shrinks to a unit interval. Once the density of corespin states $\Gamma_{N_p}(u)$ has been determined, the integration over the corespin states can be carried out.

The thermal probability density $p(u|\beta)$ in Eq. (20) contains two competing factors. The density of corespin states $\Gamma_{N_p}(u)$ peaks near $u=2/3$ and decreases algebraically to zero as u approaches the bounds of the unit interval. A tendency towards ferromagnetic (antiferromagnetic) order is reflected by an exponential increase of the Boltzmann factor towards $u=1$ ($u=0$). This factor becomes increasingly important with decreasing temperature. In the ferromagnetic

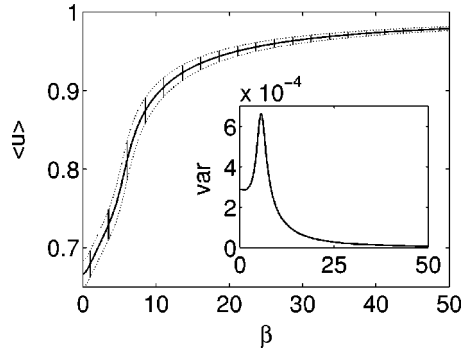

FIG. 1. Mean $\langle u \rangle$ (solid line) and standard deviation (dashed line) of $p(u|\beta)$ vs inverse temperature for a 4^3 cluster at quarter filling. The β dependence of the variance is depicted in the inset.

case, the combined distribution has its peak, depending on the value of β, somewhere between 2/3 and 1 (see Fig. 1 for an illustration in three dimensions). With increasing β, the peak shifts towards $u=1$.

In summary, the configuration space of the corespins is reduced to the one-parametric space of the UHA parameter u. This simplification is based on the assumption that as far as the Boltzmann factor is concerned, the effect of the corespins on the electrons can be replaced by a mean effective hopping. Fluctuations of the corespins are allowed for by the density $\Gamma_{N_p}(u)$ and by fluctuations of the UHA parameter, resulting in a finite lifetime of the quasiparticles even in the FM phase, and in a finite bandwidth even in the antiferromagnetic phase. The density $\Gamma_{N_p}(u)$ takes care of the correct inclusion of the corespin entropy, which will become crucial in the ensuing discussion.

Validity of the additional approximation. In order to assess the additional approximation introduced by the substitution of the terms $\langle \sin^2(\vartheta/2) \rangle \approx 1-\langle \cos \vartheta/2 \rangle^2 \equiv 1-u^2$ and $\langle \cos \vartheta \rangle \approx 2\langle \cos \vartheta/2 \rangle^2 - 1 \equiv 2u^2-1$, a Monte Carlo simulation with random spins on a 16^3 simple cubic (sc) lattice has been performed. For each spin configuration, the mean values of the functions $\cos(\vartheta/2)$, $\cos(\vartheta)$, and $\sin^2(\vartheta/2)$ have been computed. The resulting scatter plot is depicted in Fig. 2. Astonishingly, the data follow a unique curve and moreover they are fairly well described by the approximation employed.

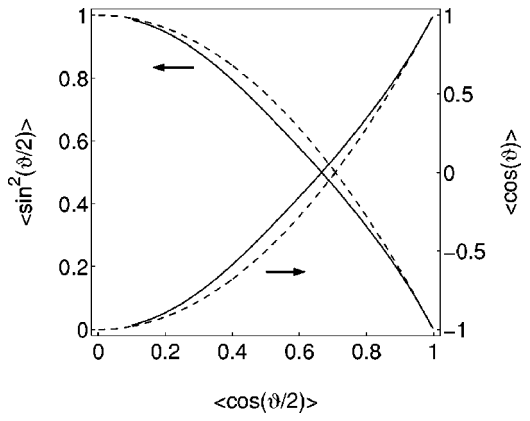

FIG. 2. Average $\langle \sin^2(\vartheta/2) \rangle$ and average $\langle \cos \vartheta \rangle$ as a function of the average hopping $u=\langle \cos \vartheta/2 \rangle$ for a 16^3 cluster. The dashed lines show the results of the approximation explained in the text.

IV. UHA VERSUS MONTE CARLO IN ONE DIMENSION

In this section, we scrutinize the uniform hopping approach by a detailed comparison of its results with MC data obtained for the original Hamiltonian, Eq. (11). Since the UHA affects only the treatment of the corespins, we will restrict our attention to a one-orbital model and neglect the degeneracy of the e_g orbitals. In this case, Hamiltonian (23) simplifies to

$$\hat{H}_p(u) = -u\sum_{\langle ij \rangle} c_i^\dagger c_j - \frac{1-u^2}{2J_H}\sum_i z_i n_i + V\sum_{\langle ij \rangle} n_i n_j + J' N_p (2u^2-1), \tag{24}$$

where z_i denotes the number of nearest neighbors of site i.

For a one-dimensional chain with open boundary condition, $\Gamma_{N_p}(u)$ can be calculated exactly. For a two-site lattice, we find $\Gamma_1(u)=2u\chi_{[0,1]}(u)$, where $\chi_B(u)$ denotes the characteristic function of the set B. Since the relative angles of the $N_p=L-1$ nearest-neighbor pairs of a chain of length L are independent, $\Gamma_{N_p}(u)$ reduces to a (N_p-1)-fold convolution of $\Gamma_1(u)$. Therefore, $\Gamma_{N_p}(u)$ is piecewise polynomial and can be evaluated numerically. It can be approximated by a Gaussian, which is not surprising because the central limit theorem applies. In combination with the Boltzmann factor, however, a Gaussian approximation is not good enough because the Boltzmann factor amplifies the tails of the distribution.

A. Energy distribution

In this section, we will compare UHA with MC results for the DE model with $V=J'=0$, $J_H=\infty$ for a one-dimensional system with one e_g orbital per site. The Hamiltonian of Eq. (24) reduces to a one-particle tight-binding Hamiltonian

$$\hat{H}_p(u) = -u\sum_{\langle i,j \rangle} c_i^\dagger c_j, \tag{25}$$

with only kinetic energy. The hopping integral u is the only remnant of the interaction with the t_{2g} corespins. The grand potential reads

$$-\beta\Omega(u) = \sum_k \ln(1+e^{-\beta(\epsilon_k-\mu)}) = \int dE \rho_L(E) \ln(1+e^{-\beta(E-\mu)}), \tag{26}$$

where the one-particle eigenvalues $\epsilon_k = -2u\cos k$ depend on u and $\rho_L(E)$ denotes the tight-binding DOS of the L-site lattice. $\Omega(u)$ can now be computed easily, and along with exact results for $\Gamma_{N_p}(u)$, we have access to the partition function and thermal quantities such as the kinetic energy. In Fig. 3, the results for the kinetic energy are compared with

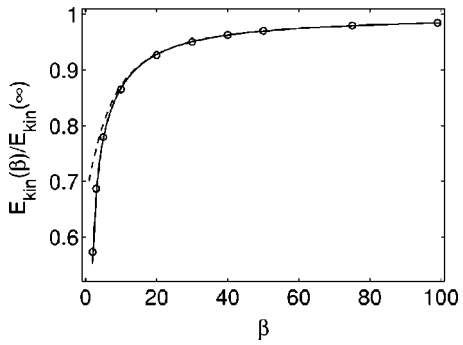

FIG. 3. Kinetic energy vs β for a 20-site Kondo chain with $J_H=\infty, J'=V=0$, and $N=10$. The statistical errors of the Monte Carlo data (circles) are smaller than the marker size. The MC data are compared with results of UHA (solid line) and the canonical low-T approximation (dashed line).

those of unbiased MC simulations. One finds an impressive agreement between the two results. The energies are reproduced within the error bars for all values of β. At higher temperatures, this agreement is not obvious at all because the corespins are strongly fluctuating. The impact of the fluctuations seems to be well described by the UHA.

For a canonical ensemble at sufficiently low temperatures (canonical low-T approximation), one can derive an analytical result for the UHA. To do so, the function $\Omega(u)$ is replaced by the ground-state energy of the tight-binding Hamiltonian, which we write as

$$\Omega(u)=uE_k, \tag{27}$$

with a factor E_k (total energy of a tight-binding system with unit hopping amplitude) independent of u. The canonical partition function then reads

$$Z=\int \mathcal{D}[\mathcal{S}]e^{-\beta u E_k}.$$

Since u can be expressed as the average $u=(1/N_p)\Sigma\cos(\vartheta_{ij}/2)$, the exponential function can be written as a product of factors containing only nn spins. In the case of a 1D chain with open boundary conditions or for a Bethe lattice, the relative angles of neighboring spins can thus be integrated independently. Consequently, the partition function factorizes and (up to some unimportant constant factors) can be transformed to

$$Z=\left(\int_0^1 du\Gamma_1(u)e^{-u\zeta}\right)^{N_p}=\left(2\frac{1-e^{-\zeta}(1+\zeta)}{\zeta^2}\right)^{N_p},$$

with $\zeta=\beta E_k/N_p$. By differentiation with respect to β, we obtain the kinetic energy

$$E_{\rm kin}=E_k\frac{\zeta^2+2\zeta+2-2e^{\zeta}}{\zeta(\zeta+1-e^{\zeta})}.$$

This result is shown as a dashed line in Fig. 3. The comparison with MC results shows an increasingly close agreement for $\beta\gtrsim 10$.

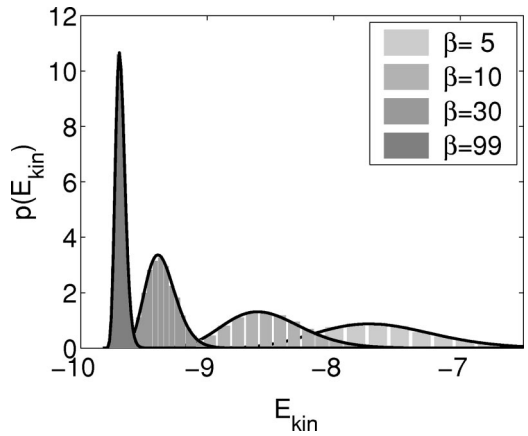

FIG. 4. Probability density for the kinetic energy of a 16-site DE chain at half filling for various values of β. The histograms are taken from unbiased Monte Carlo data. Solid lines represent UHA results.

The above considerations show that UHA on the average correctly describes the kinetic processes. In order to give a more critical assessment of UHA, we study the fluctuations of the kinetic energy. It should be kept in mind that the motivation of UHA is to describe the mean energy correctly. It is thus not *a priori* obvious whether UHA also properly reflects its fluctuations. In UHA, the fluctuations of the kinetic energy are exclusively due to fluctuations of the uniform hopping parameter u, that in turn is related to the relative nn angles of corespins. In the full model, however, the relative nn angles fluctuate locally.

By sampling the contributions to the kinetic energy in a MC simulation including local fluctuations, we obtain histograms for the full model. They can be compared with the statistical distribution of the kinetic energy corresponding to the UHA density $\Gamma_{N_p}(u)e^{-\beta\Omega(u)}$. The result of this comparison is depicted in Fig. 4. We find a perfect agreement between MC and UHA results revealing a nontrivial justification of UHA.

B. Spectral function and Coulomb correlations

We will now comment on the influence of the nn Hubbard interaction on the spectral density and compare MC with UHA results. A thorough discussion of correlation effects in conjunction with the Kondo model will be given elsewhere.[24] We have studied a 12-site chain with open boundaries at half filling of the effective spinless model, i.e., quarter filling of the original Kondo model. In this case the implementation of the ESF model reduces the dimension of the Lanczos basis from $\binom{2L}{N}=134\,596$ to $\binom{L}{N}=924$. Additionally, UHA replaces the sampling of spin configurations with a simple scan in the UHA parameter u (several 100 000 spin configurations in MC vs ≈ 20 values of u in the relevant u range $[0.8,1.0]$ in UHA).

Without the Hubbard interaction, the system is ferromagnetic due to the DE mechanism. The spectral density, calculated by MC and depicted in Fig. 12 of Ref. 18, is that of a

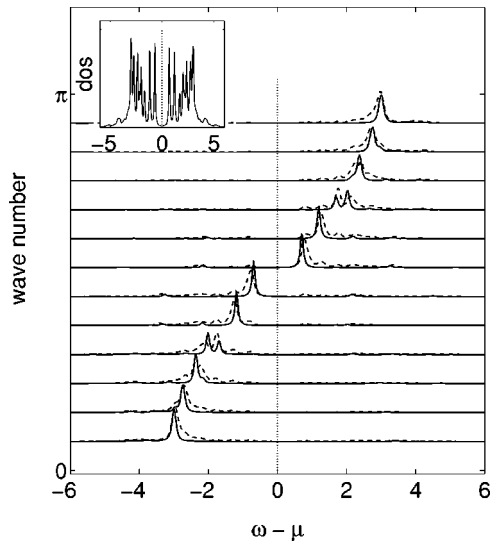

FIG. 5. Spectral density of a 12-site Kondo chain at quarter filling ($N=6$) with $V=2$, $J'=0.02$, $J_H=6$, $\beta=50$. Data of the Monte Carlo–Lanczos hybrid algorithm (dashed lines) are compared with UHA results (solid line). The inset displays the DOS obtained from MC simulations.

tight-binding model.[10] The peaks are slightly broadened due to spin fluctuations. In UHA, through the variation of the uniform hopping amplitude u, we obtain a superposition of tight-binding bands that combine to a broadened tight-binding band. For the parameters $L=20$, $J_H=6$, and $J'=0.02$ and at $\beta=50$, the average uniform hopping amplitude $\langle u\rangle$ is found to be $\langle u\rangle\simeq 0.953$. This yields a band width W of $W\simeq 3.8$, which agrees with what we have found in MC simulations.

We now include the nn Hubbard term with $V=2$ in the ESF model Eq. (11), or alternatively in the UHA Hamiltonian in Eq. (23). The Monte Carlo data are obtained by resorting to a Lanczos exact diagonalization scheme for each corespin configuration. The fermionic trace is then evaluated by summing over enough lowest eigenstates, such that convergence is ensured. Details will be given elsewhere.[24]

In UHA, a $t-V$ model has to be diagonalized. The Lanczos diagonalization for this model is not really faster than the diagonalization of the original model, but the configuration space is drastically reduced, as only the parameter u has to be sampled within the unit interval $u\in[0,1]$.

Figure 5 shows the spectral density derived by both approaches. The electronic correlation has important impact on the spectral density. A gap appears in the middle of the original Brillouin zone at $k=\pi/2$, indicating the doubling of the unit cell due to charge ordering. In addition, the spectra exhibit more structure than just a simple quasiparticle peak.

This result is neither new nor surprising. The point we want to make here is that UHA works well also for correlated electrons, indicating that it can reliably be employed to study more sophisticated and more realistic models for the manganites, e.g., by including correlation effects, phononic degrees of freedom, and more orbital degrees of freedom.

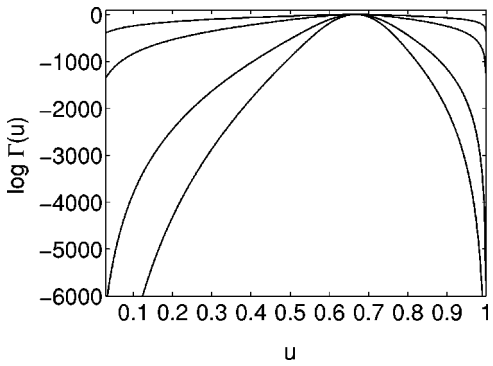

FIG. 6. Density of corespin states $\Gamma_{N_p}(u)$ vs UHA parameter u for an sc lattice with linear size $L_x=4$ (top), $L_x=6,10$, and $L_x=12$ (bottom). All curves peak near $u=2/3$, as in the 1D case.

V. FM PHASE TRANSITION IN THREE DIMENSIONS

We now apply UHA to an sc crystal and determine the Curie temperature for the bare one-orbital DE model. The crucial difference between the 1D and the 3D geometry is that in the latter the relative angles of nn corespin pairs are in general correlated. Therefore, the correct density $\Gamma_{N_p}(u)$ is no longer a convolution of the density $\Gamma_1(u)$ of a single spin pair.

A. Determination of $\Gamma_{N_p}(u)$

In order to determine $\Gamma_{N_p}(u)$ for a 3D geometry, we have to resort to numerical approaches. We have employed the Wang-Landau algorithm[25] with single spin-flip updates, which was invented for the determination of the density of states of classical models. Figure 6 shows the resulting density $\Gamma_{N_p}(u)$ as a function of u for an sc lattice with linear dimensions $L_x=4,6,10$, and 12. As in the one-dimensional case, $\ln[\Gamma_{N_p}(u)]$ diverges as $u\to 0$ and $u\to 1$. In fact, one can show that

$$\ln[\Gamma_{N_p}(u)] \overset{u\to 1}{\to} (L-1)\ln(1-u) \tag{28}$$

in any spatial dimension. This divergence has important impact on the low-temperature thermodynamic behavior. The entropy diverges logarithmically and the specific heat has a finite value for $T\to 0$. The scale in Fig. 6 might appear exaggerated, but it is actually the small tail close to $u=1$ which will become important for low temperatures.

The computational effort of finite-temperature UHA is now essentially reduced to the Wang-Landau determination of $\Gamma_{N_p}(u)$, while the integration over u to calculate various physical results takes only a small amount of computer time. Therefore, results can be obtained for much larger lattices than with the conventional MC approach and, indeed, for a whole range of temperatures at once.

B. FM to PM transition at $J_H=\infty$, $J'=0$

We now study the 3D DE model in the UHA. Based on the tests of the preceding section, we expect the UHA results

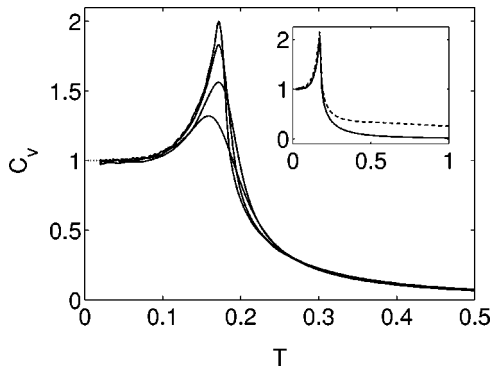

FIG. 7. Specific heat per site of the sc DE model at $n=0.5$ ($\mu=0$) vs temperature for $L=4^3$ (bottom), $L=6^3,10^3$, and $L=16^3$ (top). Parameters are $J_H=\infty, J'=0$. The results are obtained by the ''canonical low-T approximation'' (see text). In the inset, the approximate result for a 16^3 lattice is compared with that of an exact grand canonical calculation (dashed line).

to be reliable also in this case. We restrict the present discussion to the case $J_H=\infty, J'=0$. For these parameters, only the FM and paramagnetic (PM) phases exist.[18,26]

The trend from PM to FM can already be seen in Fig. 1, where we show the expectation value $\langle u\rangle$ of the uniform hopping parameter and its standard deviation as a function of the inverse temperature β at $\mu=0$. Already for a relatively small system, $p(u|\beta)$ is sharply peaked. Starting from $u=2/3$ at high temperatures, the expectation value $\langle u\rangle$ tends towards unity, i.e., FM corespins, as $\beta\to\infty$. From Eq. (28), we find the asymptotic formula

$$u^*=1+\frac{1}{\beta\epsilon_k} \tag{29}$$

for the position u^* of the maximum of $p(u|\beta)$, where ϵ_k denotes the kinetic energy per lattice site of the tight-binding model with unit hopping parameter. It turns out that for $\beta\gtrsim 10$, the curves for u^* and $\langle u\rangle$ coincide. Well above this temperature, near $\beta\approx 5.5$, the variance of $p(u|\beta)$ shows a peak (see inset of Fig. 1), indicating important fluctuations near this temperature. For the determination of the Curie temperature of the DE model, we study the specific heat C_v as a function of temperature for various system sizes. The peaks of the specific heat at quarter filling ($n=0.5$) are plotted in Fig. 7. They show signs of divergence as the lattice size increases. This indicates the presence of a second-order phase transition from FM to PM. We identify the position $T^*\simeq 0.17$ of the peak as the phase-transition temperature T_C at $n=0.5$. This value is somewhat higher than that determined with the hybrid MC algorithm[16] ($T_C\simeq 0.14$) for a 16^3, lattice but is better than the variational estimate[27] $T_C\simeq 0.19$.

In order to facilitate the calculation, particularly for electron fillings different from $n=0.5$ ($\mu=0$), we consider a canonical ensemble and replace the Boltzmann factor by $e^{-\beta F}$. If the temperature is small on the electronic energy scale, we can replace the electronic free energy F by the ground-state energy $F\simeq uE_k$. As introduced above, E_k denotes the kinetic energy at $T=0$ of the tight-binding model with unit hopping amplitude (now in three dimensions) for a given electron filling. This approximation is justified because $T_C\lesssim 0.17$ is indeed small enough. The partition function now reads

$$Z=\int_0^1 du\,\Gamma_{N_p}(u)e^{-\beta E_k u}. \tag{30}$$

The impact of this ''canonical low-T approximation'' is illustrated in the inset of Fig. 7. We find that the position of the peak is not affected at all. The only difference to the full grand canonical result is the longer tail at higher temperatures of the full result, which is due to additional fluctuations of the electrons.

The specific heat approaches a constant value $C_v=1$ as $T\to 0$. This can be inferred from Eq. (29), since, for low temperatures, the internal energy per lattice site is given by $\epsilon_k u^*$ whose derivative with respect to temperature exactly yields unity. This explains the plateau of C_v for $T\lesssim 0.1$.

Signatures of the FM to PM phase transition should show up especially in the magnetic susceptibility[12] χ. For its calculation, the density $\Gamma_{N_p}(u)$ is not sufficient because a value u of the average hopping does not determine the magnetization m. Given the conditional probability $p(m|u)$, the moments of the magnetization are

$$\langle|m|^n\rangle\equiv\frac{1}{\mathcal{Z}}\int_0^1 du\,\Gamma_{N_p}(u)e^{-\beta\Omega(u)}M^{(n)}(u)$$

with

$$M^{(n)}(u)=\int_0^1 dm|m|^n p(m|u).$$

Estimates of the conditional moments $M^{(n)}(u)$ have been obtained in a second run of the Wang-Landau algorithm. A random walk in the space of all corespin configurations is performed whose acceptance is controlled by $1/\Gamma_{N_p}(u)$. An estimator of the susceptibility[28,29] is then given by

$$\chi=\beta L(\langle m^2\rangle-\langle|m|\rangle^2).$$

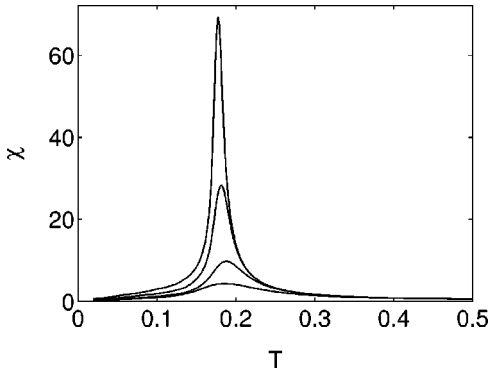

FIG. 8. Magnetic susceptibility of the sc DE model at quarter filling ($n=0.5$) vs temperature for lattice sizes 4^3 (bottom), $6^3,10^3$, and 16^3 (top). Parameters are $J_H=\infty, J'=0$. The results are obtained by the canonical low-T approximation.

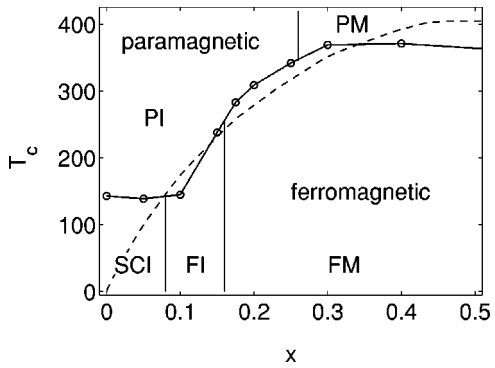

FIG. 9. Curie temperature (dashed line) of the one-orbital DE model for a 16^3 cluster and $t=0.2$ eV. Circles and phases PM, PI, FM, FI, and SCI are experimental results[32] for $La_{1-x}Sr_xMnO_3$.

Figure 8 shows the susceptibility as a function of the temperature for various lattice sizes. We observe clear signs of a divergence near $T\simeq 0.18$ which corroborates the transition temperature obtained from the specific heat.

The filling dependence of T_C is easily determined from Eq. (30). Since the filling dependence only enters via E_k, which shows up in combination with β, we have the simple relation

$$\beta_c E_k = \text{const}$$

for the transition temperature. Thus, the Curie temperature T_C is proportional to the kinetic energy E_k of the tight-binding model which, in turn, is a function of the electron filling. The proportionality of T_C to the bandwidth has already been found based on different approximations.[13,30,31]

In order to compare our calculations with experimental results, we fix the single free parameter in the DE model, i.e., the hopping amplitude. We choose $t=0.2$ eV, a value reasonable for the material.[22] The dashed line of Fig. 9 shows the Curie temperature obtained from the DE model in UHA. We find an astonishingly good agreement to the experimentally observed phase diagram of $La_{1-x}Sr_xMnO_3$ in the ferromagnetic regime. Our result is in sharp contrast to the claim made by Millis *et al.*[19] that the DE model cannot even explain the right order of magnitude of T_C for the manganites. The reasoning of Ref. 19 starts from similar ideas as the UHA but is based on additional uncontrolled approximations. Our results for the DE model are in accord with other estimates.[11,13,20]

The experimentally observed phase diagram shows additional phases for small concentrations: ferromagnetic insulating (FI), paramagnetic insulating (PI), and a spin-canting insulating (SCI) state. These states are not accounted for in our present approach. For a correct description, a finite value of J' is important, as well as generalizations of UHA, which will be discussed elsewhere.[24]

VI. CONCLUSIONS

In this paper, we have presented the uniform hopping approach (UHA) for the FM Kondo model at finite temperature. We have used our method to calculate the ferromagnetic to paramagnetic phase-transition temperature of the one-orbital DE model for large 3D systems. We find that the DE model yields a Curie temperature that is comparable to the experimental data.

The finite temperature UHA in the frame of the ESF model reduces the numerical effort of a simulation by several orders of magnitude, while retaining all crucial physical features. In the example given in Sec. IV B, the reduction factor is at least 10^6. The key idea is to map the physics of the high-dimensional configuration space of the t_{2g} corespins onto an effective one-parametric model. The density of states entering our approach can be determined by the Wang-Landau algorithm. A full thermodynamic evaluation of the UHA model takes into account entropy and fluctuations of the corespins. Tests for 1D systems reveal that UHA results are in close agreement with unbiased MC data for static and dynamic observables.

This reduction in numerical effort will allow us to include phononic and/or orbital degrees of freedom in future numerical simulations in order to study more realistic models for the manganites.

ACKNOWLEDGMENTS

This work has been supported by the Austrian Science Fund (FWF), Project No. P15834-PHY. We are indebted to W. Nolting for stimulating discussions and to V. Martín-Mayor for drawing our attention to Refs. 16, 17, and 27.

*Electronic address: koller@itp.tu-graz.ac.at

[1] T. Kaplan and S. Mahanti, *Physics of Manganites*, 1st ed. (Kluwer Academic Plenum, New York, 1999).
[2] E.L. Nagaev, *Colossal Magentoresistance and Phase Separation in Magnetic Semiconductors*, 1st ed. (Imperial College Press, London, 2002).
[3] P. Horsch, J. Jaklič, and F. Mack, Phys. Rev. B **59**, R14 149 (1999).
[4] J. Bala, A.M. Oles, and P. Horsch, Phys. Rev. B **65**, 134420 (2002).
[5] C. Zener, Phys. Rev. **82**, 403 (1951).
[6] D.M. Edwards, Adv. Phys. **51**, 1259 (2002).
[7] D. Meyer, C. Santos, and W. Nolting, J. Phys.: Condens. Matter **13**, 2531 (2001).
[8] W. Müller and W. Nolting, Phys. Rev. B **66**, 085205 (2002).
[9] E. Dagotto, S. Yunoki, A.L. Malvezzi, A. Moreo, J. Hu, S. Capponi, D. Poilblanc, and N. Furukawa, Phys. Rev. B **58**, 6414 (1998).
[10] S. Yunoki and A. Moreo, Phys. Rev. B **58**, 6403 (1998).
[11] S. Yunoki, J. Hu, A.L. Malvezzi, A. Moreo, N. Furukawa, and E. Dagotto, Phys. Rev. Lett. **80**, 845 (1998).
[12] H. Yi, N.H. Hur, and J. Yu, Phys. Rev. B **61**, 9501 (2000).
[13] N. Furukawa, *Physics of Manganites*, 1st ed. (Kluwer Academic, New York, 1999).
[14] Y. Motome and N. Furukawa, J. Phys. Soc. Jpn. **69**, 3785 (2000).
[15] A. Chattopadhyay, A.J. Millis, and S. Das Sarma, Phys. Rev. B **64**, 012416 (2001).
[16] J.L. Alonso, L.A. Fernández, F. Guinea, V. Laliena, and V.

Martín-Mayor, Nucl. Phys. B **569**, 587 (2001).
[17] J.L. Alonso, J.A. Capitán, L.A. Fernández, F. Guinea, and V. Martín-Mayor, Phys. Rev. B **64**, 054408 (2001).
[18] W. Koller, A. Prüll, H.G. Evertz, and W. von der Linden, Phys. Rev. B **66**, 144425 (2002).
[19] A.J. Millis, P.B. Littlewood, and B.I. Shraiman, Phys. Rev. Lett. **74**, 5144 (1995).
[20] H. Röder, R.R.P. Singh, and J. Zang, Phys. Rev. B **56**, 5084 (1997).
[21] P.-G. de Gennes, Phys. Rev. **118**, 141 (1960).
[22] E. Dagotto, T. Hotta, and A. Moreo, Phys. Rep. **344**, 1 (2001).
[23] W. von der Linden and W. Nolting, Z. Phys. B: Condens. Matter **48**, 191 (1982).
[24] W. Koller, A. Prüll, H. G. Evertz, and W. von der Linden (unpublished).
[25] F. Wang and D.P. Landau, Phys. Rev. Lett. **86**, 2050 (2001); Phys. Rev. E **64**, 056101 (2001).
[26] J. van den Brink and D. Khomskii, Phys. Rev. Lett. **82**, 1016 (1999).
[27] J.L. Alonso, L.A. Fernández, F. Guinea, V. Laliena, and V. Martín-Mayor, Phys. Rev. B **63**, 054411 (2001).
[28] K. Binder and E. Luijten, Phys. Rep. **344**, 179 (2001).
[29] K. Binder and D. W. Heermann, *Monte Carlo Simulation in Statistical Physics—An Introduction* (Springer, Berlin, 1988).
[30] Y.A. Izyumov and M.V. Medvedev, Sov. Phys. JETP **32**, 302 (1971).
[31] W. Nolting (private communication).
[32] A. Urushibara, Y. Moritomo, T. Arima, A. Asamitsu, G. Kido, and Y. Tokura, Phys. Rev. B **51**, 14 103 (1995).